

Resonator-based all-optical Kerr-nonlinear phase shifting: Design and limitations

Gino Priem,^{a)} Inge Notebaert, Peter Bienstman, Geert Morthier, and Roel Baets
*Department of Information Technology (INTEC), Ghent University, Sint-Pietersnieuwstraat 41,
 9000 Ghent, Belgium*

(Received 9 June 2004; accepted 12 October 2004; published online 23 December 2004)

The design of all-optical phase shifting by means of Kerr-nonlinear resonators is investigated using a one-dimensional analytical model. Dependence on different device parameters and design optimization are discussed. In particular, it is shown that a tradeoff in terms of optical input power and device length is required, which is limited by the signal bandwidth. © 2005 American Institute of Physics. [DOI: 10.1063/1.1829148]

I. INTRODUCTION

From the beginning, nonlinear optics showed great potential for all-optical signal processing, because of its ultrafast response times. However, nonlinear effects like the Kerr effect are typically very small in standard photonic material systems ($n_2 \approx 10^{-15} - 10^{-13} \text{ cm}^2/\text{W}$). This means that very high input powers or very long device lengths are required to obtain a phase shift of π —which is the basis for most optical switches today—leading to unpractical designs.

A possible route to overcome these impairments is by using resonating structures. They enhance the electric field or power density and slow down the pulse propagation, so that the nonlinear response is larger. Examples of such structures are coupled cavity waveguides, ring resonators,¹... It has been shown that with these components, important improvements are possible for the purpose of Kerr-nonlinear phase shifting.¹⁻³ In addition, they also exhibit features which cannot be implemented with simple waveguides, such as all-optical limiting,⁴ all-optical switching, and bistability.⁵⁻¹⁰

An important question however is how far one can go in reducing the input power or device length. Increasing the resonating effect will result in further reduction, however, at the expense of the obtainable signal bandwidth since stronger resonators have a higher finesse. Therefore a tradeoff among input power, device length, and signal bandwidth is to be expected.

In this paper, a detailed analysis of one-dimensional (1D) coupled resonators is performed to investigate the realistic possibilities of resonator-based approaches for Kerr-nonlinear phase shifting in case the data signal itself behaves either linearly or nonlinearly. A 1D model makes an analytical description of the nonlinear effects inside the structure possible, providing deeper insight in the influence of various structural parameters. Although this model essentially considers a nonlinear Fabry–Perot cavity,¹⁰ it is used here in the context of waveguide-implemented devices. Based on this model, general conclusions are drawn about design aspects which are representative for all three-dimensional (3D) structures mentioned above and design optimization is carried out

to determine the limitations of this approach. Note also that this 1D structure is an immediate model for Fabry–Perot cavities implemented in waveguides.

The organization of this paper is as follows. In Sec. II the resonator structure considered in this paper is discussed. Sections III and IV describe the linear and nonlinear behavior of this structure. The applicability of resonator structures is then discussed in Sec. V. Finally conclusions are drawn in Sec. VI.

II. 1D STRUCTURE

The resonator structure that will be used throughout this paper has the following period;

$$a_{\lambda_c/8} b_{\lambda_c/4} a_{\lambda_c/4} b_{\lambda_c/4} \dots b_{\lambda_c/4} a_{N_{\text{cav}} \times \lambda_c/2} b_{\lambda_c/4} a_{\lambda_c/4} b_{\lambda_c/4} \dots b_{\lambda_c/4} a_{\lambda_c/8},$$

mirror
cavity
mirror

with a and b two different materials, λ_c the resonance wavelength of the structure, and N_{cav} an integer indicating the cavity length (in units of $\lambda_c/2$). The parameter N_{dbr} will be used to indicate the total number of b layers in one resonator period. The length of one resonator period is then

$$L_{\text{per}} = \frac{\lambda_c}{4n_a} (N_{\text{dbr}} - 1 + 2N_{\text{cav}}) + \frac{\lambda_c}{4n_b} (N_{\text{dbr}}). \quad (1)$$

Quarter-wave mirrors were chosen here for analytical purposes and because they have the largest reflectivity per unit of length. The rightmost layer of one period combines with the leftmost of the next period to create an uninterrupted distributed Bragg reflector (DBR) mirror. The in- and out-coupling layers to the resonator structure are assumed to have a refractive index n_a .

An example for two periods is given in Fig. 1.

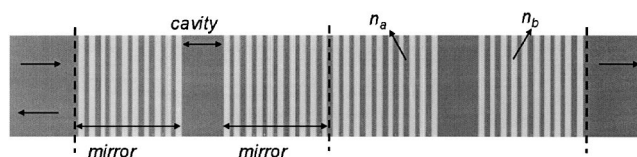


FIG. 1. Two period resonator structure with in- and out-coupling layer. Refractive indices are indicated.

^{a)}Electronic mail: gino.priem@ugent.be

III. LINEAR THEORY

The linear properties for a resonating structure with one and with ∞ periods are now derived. These two cases serve as boundaries for the realistic situation in which the number of periods to achieve a nonlinear phase shift of π will be finite, but still can be either low or high.

A. Properties of one period

A rigorous calculation using the transfer-matrix method is in principle possible but is not suitable to derive the analytical formulae. Therefore a few approximations are introduced. The frequency dependence of the amplitude of mirror transmission and reflection coefficients t_{dbr} and r_{dbr} can generally be neglected compared to that of the phase, so

$$t_{\text{dbr}} = |t_{\text{dbr}}| e^{j\varphi_t} \approx |t_{\text{dbr}}|_{\nu_c} e^{j\varphi_t}, \quad (2)$$

$$r_{\text{dbr}} = |r_{\text{dbr}}| e^{j\varphi_r} \approx |r_{\text{dbr}}|_{\nu_c} e^{j\varphi_r}. \quad (3)$$

For the mirrors defined in this paper, one has

$$|t_{\text{dbr}}|_{\nu_c} = \frac{2n_a^{N_{\text{dbr}}/2} n_b^{N_{\text{dbr}}/2}}{n_a^{N_{\text{dbr}}} + n_b^{N_{\text{dbr}}}}, \quad (4)$$

$$|r_{\text{dbr}}|_{\nu_c} = \frac{n_a^{N_{\text{dbr}}} - n_b^{N_{\text{dbr}}}}{n_a^{N_{\text{dbr}}} + n_b^{N_{\text{dbr}}}}. \quad (5)$$

Using a linear approximation, the phases φ_t and φ_r can be written as

$$\varphi_t = \pm \frac{\pi}{2} + \left. \frac{d\varphi_t}{d\nu} \right|_{\nu_c} (\nu - \nu_c), \quad (6)$$

$$\varphi_r = 0 + \left. \frac{d\varphi_r}{d\nu} \right|_{\nu_c} (\nu - \nu_c), \quad (7)$$

with the sign of φ_t depending on N_{dbr} and $d\varphi_t/d\nu|_{\nu_c} = d\varphi_r/d\nu|_{\nu_c} \equiv d\varphi/d\nu|_{\nu_c}$ due to the symmetry of the mirror. An analytical expression for $d\varphi/d\nu|_{\nu_c}$ will be determined in Sec. III B.

If the resonator is now considered as the aggregate of a cavity, two mirror sections and two outside layers (for continuity) and the transfer-matrix approach is applied, the transmission coefficient for the complete structure becomes

$$t_{\text{tot}}(\nu) = \frac{e^{-j\varphi_{\text{cav}} + 2j\varphi_t - j(\pi/2)(\nu/\nu_c)} |t_{\text{dbr}}|_{\nu_c}^2}{1 + e^{2j\varphi_t - 2j\varphi_{\text{cav}}} |r_{\text{dbr}}|_{\nu_c}^2} \quad (8)$$

with $\varphi_{\text{cav}} = \pi N_{\text{cav}}(\nu/\nu_c)$ the phase length of the cavity and the factor $e^{-j(\pi/2)(\nu/\nu_c)}$ corresponding to the phase change in the in- and out-coupling sections (together with a quarter wavelength, see Sec. II). Using Eqs. (6) and (7) and expanding the exponentials in the denominator around $\nu = \nu_c$, the intensity transmission $|t_{\text{tot}}(\nu)|^2$ and the phase change $\phi(\nu)$ over a single resonator period for a resonator structure with one period become

$$|t_{\text{tot}}(\nu)|^2 \approx \frac{1}{1 + \frac{4(\nu - \nu_c)^2}{|t_{\text{dbr}}|_{\nu_c}^4} \left(N_{\text{cav}} \frac{\pi}{\nu_c} - \left. \frac{d\varphi}{d\nu} \right|_{\nu_c} \right)^2}, \quad (9)$$

$$\phi^{(1)}(\nu) \approx \pm \frac{\pi}{2} - \arctan \left[\frac{2(\nu - \nu_c)}{|t_{\text{dbr}}|_{\nu_c}^2} \left(N_{\text{cav}} \frac{\pi}{\nu_c} - \left. \frac{d\varphi}{d\nu} \right|_{\nu_c} \right) \right]. \quad (10)$$

Equation (9) shows the typical Lorentzian transmission characteristic of a single resonator, while Eq. (10) shows that its output phase relation has an arctan behavior. Note that $d\varphi/d\nu|_{\nu_c}$ still needs to be determined. This will be done in Sec. III B.

B. Bloch characteristics (properties for ∞ periods)

Using the Floquet–Bloch theory, the general dispersion relation—which relates the propagation constant k of a Bloch mode to its frequency ν —for a structure with a period consisting of N layers (indicated by $a \cdots N$) is given by

$$\begin{aligned} & 2^{N+1} n_a n_b \cdots n_N \cos(kL_{\text{per}}) \\ &= \sum_{p_a \cdots p_N=0}^1 (-1)^{p_a + \cdots + p_N} \cos[(-1)^{p_a} k_a l_a \\ & \quad + \cdots + (-1)^{p_N} k_N l_N] [(-1)^{p_a} n_a + (-1)^{p_b} n_b] \\ & \quad \times [(-1)^{p_b} n_b (-1)^{p_c} n_c] \cdots [(-1)^{p_N} n_N + (-1)^{p_a} n_a], \quad (11) \end{aligned}$$

with n_i the refractive index of layer i , $k_i = (2\pi\nu/c)n_i$, l_i the length of layer i , k the propagation constant of the Bloch mode, and $L_{\text{per}} = \sum l_i$ the period length. This formula was obtained by induction. In the case of the resonator period described above, this formula is not immediately usable because there are too many layers involved. The dispersion relation for weakly coupled resonators is however approximately sinusoidal around the central frequency ν_c ,¹¹ so it can be written as

$$\nu - \nu_c \approx - \frac{\Delta\nu}{2} \sin\left(kL_{\text{per}} \pm \frac{\pi}{2}\right), \quad (12)$$

with $\Delta\nu$ the resonance bandwidth. The exact sign depends on N_{cav} and N_{dbr} , but is not important here. kL_{per} is the phase change between the input and output over a single period, denoted as ϕ in Sec. III A. Using this notation, one obtains for the single period phase change of a resonator structure with ∞ periods,

$$\phi^{(\infty)}(\nu) \pm \frac{\pi}{2} \approx - \arcsin\left[\frac{2}{\Delta\nu}(\nu - \nu_c)\right]. \quad (13)$$

Differentiation of Eq. (13) to the frequency shows

$$\left| \frac{d\phi^{(\infty)}}{d\nu} \right|_{\nu_c} = \frac{2}{\Delta\nu}, \quad (14)$$

leading to

$$\phi^{(\infty)}(\nu) \pm \frac{\pi}{2} \approx -\arcsin \left[\left| \frac{d\phi^{(\infty)}}{d\nu} \right|_{\nu_c} (\nu - \nu_c) \right]. \quad (15)$$

An analytical expression for $|d\phi^{(\infty)}/d\nu|_{\nu_c}$ can be obtained from Eq. (11). The calculation is straightforward but very tedious. Finally one obtains

$$\left| \frac{d\phi^{(\infty)}}{d\nu} \right|_{\nu_c} = \frac{\pi}{2\nu_c |t_{\text{dbr}}|_{\nu_c}^2} \left[(1 + |r_{\text{dbr}}|_{\nu_c}^2)(2N_{\text{cav}} - 1) + 2|r_{\text{dbr}}|_{\nu_c} \frac{n_a + n_b}{n_a - n_b} \right]. \quad (16)$$

Equations (14)–(16) fully describe the resonance bandwidth and the phase relation inside the bandwidth.

C. Comparison between 1 and ∞ periods

The limiting cases of one and ∞ periods coincide for $\nu = \nu_c$. Indeed for the resonance frequency, the transmission of every single resonator period is one, so they cannot interact. Based on this, a relation for $(d\phi/d\nu)_{\nu_c}$ —which was left undetermined in Sec. III A—can be derived by an expansion of Eqs. (10) and (15) at $\nu = \nu_c$. The result of this is

$$-\frac{d\phi}{d\nu} \Big|_{\nu_c} \approx -\frac{\pi}{2\nu_c} \left(|r_{\text{dbr}}|_{\nu_c} \frac{n_a + n_b}{n_a - n_b} - 1 \right). \quad (17)$$

Substitution of this Eq. in (10) allows now to derive the output phase relation for the case of one resonator period (Sec. III A) as

$$\phi^{(1)}(\nu) \approx \pm \frac{\pi}{2} - \arctan \left[\left| \frac{d\phi^{(\infty)}}{d\nu} \right|_{\nu_c} (\nu - \nu_c) \right]. \quad (18)$$

Differentiation shows that

$$\left| \frac{d\phi^{(1)}}{d\nu} \right|_{\nu_c} = \left| \frac{d\phi^{(\infty)}}{d\nu} \right|_{\nu_c} \equiv \left| \frac{d\phi}{d\nu} \right|_{\nu_c}, \quad (19)$$

so that Eqs. (15) and (18) finally become

$$\phi^{(1)}(\nu) \approx \pm \frac{\pi}{2} - \arctan \left[\left| \frac{d\phi}{d\nu} \right|_{\nu_c} (\nu - \nu_c) \right], \quad (20)$$

$$\phi^{(\infty)}(\nu) \approx \pm \frac{\pi}{2} - \arcsin \left[\left| \frac{d\phi}{d\nu} \right|_{\nu_c} (\nu - \nu_c) \right]. \quad (21)$$

IV. NONLINEAR THEORY

The nonlinear effect on the transmission spectrum of a resonating structure can qualitatively be described as follows. The incoming light builds up inside the cavity and partially in the mirrors and therefore changes the refractive index of the complete structure. This means that both the resonance peak and the resonance bandwidth can change. The index changes also affect the output phase relation $\phi(\nu)$. In the most general case, $n_{a,2} \neq n_{b,2}$. It can then roughly be said that the resonance shift is determined by the overall value of n_2 (a shift to higher frequencies occurs for $n_2 < 0$ and vice versa), while the change of bandwidth is due to the modulation of n_2 .

In this paper, it will be assumed that $n_{a,2} \approx n_{b,2}$, which is especially a good approximation for waveguide-implemented Fabry–Perot cavities. It also holds quite well for other resonator types. This means that the resonance bandwidth can in good approximation be considered as constant (only in cases in which $n_{a,2}$ and $n_{b,2}$ have opposite signs, bandwidth changes become important). A method to calculate cases with $n_{a,2} \neq n_{b,2}$ will be discussed in Sec. IV C.

From Eqs. (15) and (18), it is obvious that the nonlinear resonance shift and the change of the output phase will be interdependent. The new resonance frequency can easily be determined by looking at the phase condition inside the cavity. From that, the nonlinear phase change will be calculated. An effort will be made to obtain insight in the nonlinear interaction, therefore avoiding long mathematical calculations as much as possible.

A. Shift of resonance frequency

From Eq. (8), it is clear that the total transmission will only be achieved if

$$\varphi_t - \varphi_{\text{cav}} = \pm \frac{\pi}{2} + p\pi, \quad (22)$$

with p any integer. In the linear case, this immediately leads to $\nu = \nu_c$, since for this frequency $\varphi_t = \pm(\pi/2)$ and $\varphi_{\text{cav}} = N_{\text{cav}}\pi$. The Kerr-nonlinear interaction will however change the refractive index in both the cavity and the mirrors, so this condition will now be true for another wavelength.

1. Kerr-nonlinear cavity only

Since the electric field will be the strongest inside the cavity, it is interesting to start by considering only the cavity as Kerr-nonlinear. First, the nonlinear enhancement in the cavity must be found. It is well known⁴ that the electric field for a certain frequency in a 1D medium with a Kerr-nonlinearity, is in good approximation given by

$$E_\nu = E_{f,\nu} e^{-j(2\pi\nu/c)[n_0 + n_2(|E_{f,\nu}|^2 + 2|E_{b,\nu}|^2)]z} + E_{b,\nu} e^{j(2\pi\nu/c)[n_0 + n_2(2|E_{f,\nu}|^2 + |E_{b,\nu}|^2)]z}, \quad (23)$$

with n_0 and n_2 the linear and nonlinear refractive indices, respectively, and $E_{f,\nu}$ and $E_{b,\nu}$ the forward and backward field components, respectively, and z the direction of propagation. An easy way to verify this is with the use of a multitime scale approach although other methods are possible. Since high-field enhancement is required, strong mirrors will typically be used in the resonating structure leading to almost perfect standing waves inside the cavity, so $E_{f,\nu} \approx E_{b,\nu} \approx E_{\text{cav},\nu}^{\text{max}}/2$ with $E_{\text{cav},\nu}^{\text{max}}$ the maximum cavity field. This means that both the forward and the backward field in Eq. (23) approximately see the same index profile, which is given by

$$n = n_0 + 3n_2 \frac{|E_{\text{max}}|^2}{4}. \quad (24)$$

Using Eqs. (4) and (5), the maximum linear cavity field for $\nu = \nu_c$ [so that $|E_{\text{in}}(\nu_c)| = |E_{\text{out}}(\nu_c)|$] for $n_a > n_b$ is given by

$$|E_{\text{cav}}^{\text{max}}(\nu_c)| = \left(\frac{n_a}{n_b}\right)^{N_{\text{dbr}}/2} |E_{\text{in}}(\nu_c)|, \quad (25)$$

with E_{in} the input field of the resonator structure. So the total refractive index inside the cavity for $\nu = \nu_c$ is simply given by

$$n = n_0 + \frac{3}{4}n_2 \left(\frac{n_{a,0}}{n_{b,0}}\right)^{N_{\text{dbr}}} |E_{\text{in}}|^2. \quad (26)$$

Together with Eqs. (10) and (11), the resonance condition (22) becomes

$$\frac{\nu}{\nu_c} = \frac{p\pi + \left.\frac{d\phi}{d\nu}\right|_{\nu_c} \nu_c}{-N_{\text{cav}}\pi \left[1 + \frac{3n_{a,2}}{4n_{a,0}} \left(\frac{n_{a,0}}{n_{b,0}}\right)^{N_{\text{dbr}}} |E_{\text{in}}|^2\right] + \left.\frac{d\phi}{d\nu}\right|_{\nu_c} \nu_c}. \quad (27)$$

Since in the linear case, the result should be $\nu = \nu_c$ and since small nonlinearities are assumed, $p = -N_{\text{cav}}$, or

$$\frac{\nu}{\nu_c} = \frac{N_{\text{cav}}\pi - \left.\frac{d\phi}{d\nu}\right|_{\nu_c} \nu_c}{N_{\text{cav}}\pi \left[1 + \frac{3n_{a,2}}{4n_{a,0}} \left(\frac{n_{a,0}}{n_{b,0}}\right)^{N_{\text{dbr}}} |E_{\text{in}}|^2\right] - \left.\frac{d\phi}{d\nu}\right|_{\nu_c} \nu_c}. \quad (28)$$

Finally, expanding both sides around their linear values, one gets

$$\frac{\Delta\nu_c}{\nu_c} = -\frac{3n_{a,2}}{4n_{a,0}} \left(\frac{n_{a,0}}{n_{b,0}}\right)^{N_{\text{dbr}}} \frac{N_{\text{cav}}}{N_{\text{cav}} - \frac{\nu_c}{\pi} \left.\frac{d\phi}{d\nu}\right|_{\nu_c}} |E_{\text{in}}|^2. \quad (29)$$

Since $d\phi/d\nu|_{\nu_c} < 0$, the resonance shift asymptotically grows to $\Delta\nu_c \rightarrow -(3/4)(n_{a,2}/n_{a,0})[(n_{a,0}/n_{b,0})]^{N_{\text{dbr}}} |E_{\text{in}}|^2 \nu_c$ for large cavities or short mirrors.

This can be explained as follows: due to the frequency dependence of the transmission and reflection phases $\varphi_t(\nu)$ and $\varphi_r(\nu)$ of the mirrors, a part of the nonlinear transmission phase change of the cavity $(3\pi/4)N_{\text{cav}}(n_{a,2}/n_{a,0}) \times [(n_{a,0}/n_{b,0})]^{N_{\text{dbr}}} \nu/\nu_c |E_{\text{in}}|^2$ is used to compensate the phase shifts $\varphi_t(\nu_c + \Delta\nu_c) - \varphi_t(\nu_c)$ and $\varphi_r(\nu_c + \Delta\nu_c) - \varphi_r(\nu_c)$. Since the frequency dependence of $\varphi_r(\nu)$ and $\varphi_t(\nu)$ is lower for shorter mirrors, the asymptotical behavior will be faster. The same holds for larger cavities since they provide a large phase change ($\propto N_{\text{cav}}$). This has an important consequence: using N_{cav} values larger than 1 could be beneficial if larger resonance shifts are needed.

2. Complete Kerr-nonlinear resonator

Deriving a formula for the resonance shift $\Delta\nu_c$ in this case is not obvious, since a large number of mirror layers are generally involved, each experiencing a different electric field and thus another Kerr-nonlinear effect. At the new resonance frequency, the field in the cavity will again be the largest of the resonator period, like it was in the linear case.

So, for a large cavity compared to the mirror sections, the resonance shift is again expected to be $\Delta\nu_c \rightarrow -(3/4) \times (n_{a,2}/n_{a,0})[(n_{a,0}/n_{b,0})]^{N_{\text{dbr}}} |E_{\text{in}}|^2 \nu_c$.

For small cavities or large mirrors, however, the resonance shift will be much larger than indicated by Eq. (29). The transition between both states is expected to be faster for smaller mirrors and thus larger refractive index contrast. It is however not possible to calculate $\Delta\nu_c$ analytically, starting from Eq. (22). To derive the resonance shift in this case, another method will be used (see Sec. IV C).

B. Shift of phase relation ϕ

The Kerr-nonlinear phase shift per period $\Delta\phi$ will now be calculated. The same approach will be used as in Sec. III: first, the limiting situations of structures with one period and with ∞ periods will be discussed. Then the results will be compared and generalized to N periods.

1. Phase shift for one period

In Sec. III A, it was shown that the linear phase relation for one period is given by

$$\phi_L^{(1)}(\nu) \approx \pm \frac{\pi}{2} - \arctan \left[\left. \frac{d\phi_L}{d\nu} \right|_{\nu_{c,L}} (\nu - \nu_{c,L}) \right]. \quad (30)$$

Since it was assumed above that the resonance bandwidth change is neglectable, one will have

$$\left. \frac{d\phi_L}{d\nu} \right|_{\nu_{c,L}} \approx \left. \frac{d\phi_{NL}}{d\nu} \right|_{\nu_{c,NL}} \equiv \left. \frac{d\phi}{d\nu} \right|_{\nu_c}. \quad (31)$$

The nonlinear frequency shift for $\nu \neq \nu_c$ will however not be equal to $\Delta\nu_c$. In general, the field profile of one resonator period for frequency ν will scale approximately with a factor $|t_{\text{tot},L}(\nu)|$ compared to ν_c . Important deviations from this only occur for frequencies for which $|t_{\text{tot},L}(\nu)|$ is very small. Typically, however, these regions are of no importance for applications. Since the Kerr effect now scales with $|E|^2$, the nonlinear frequency shift in case $\nu \neq \nu_c$ becomes

$$\Delta\nu_{NL} \approx |t_{\text{tot},L}(\nu)|^2 \Delta\nu_c, \quad (32)$$

which means that the general Kerr-nonlinear phase relation for one period is in good approximation given by

$$\phi_{NL}^{(1)}(\nu') = \phi_L^{(1)}(\nu), \quad (33)$$

with $\nu' = \nu + |t_{\text{tot},L}(\nu)|^2 \Delta\nu_c$. In general, however, one will be interested in the phase shift in the neighborhood of the resonance peaks [*e.g.*, $\nu' = \nu_{c,L} + \nu_{c,NL}/2$]. The equality

$$\nu + |t_{\text{tot},L}(\nu)|^2 \Delta\nu_c = \frac{\nu_{c,L} + \nu_{c,NL}}{2} \quad (34)$$

has a single real solution $\nu = \nu_{\text{sol}}$, which also gives $|t_{\text{tot},L}(\nu_{\text{sol}})|^2$ required to calculate $\phi_{NL}^{(1)}(\nu_{c,L} + \nu_{c,NL}/2)$. This $\nu = \nu_{\text{sol}}$ is a complicated formula as is $|t_{\text{tot},L}(\nu_{\text{sol}})|^2$, but for low-frequency shifts, $|t_{\text{tot},L}(\nu_{\text{sol}})|^2 \approx 1$ will be a relative good approximation. In this case, the phase shift $\Delta\phi^{(1)}$ —calculated at $\nu = \nu_{c,L} + \nu_{c,NL}/2$ —will be given by

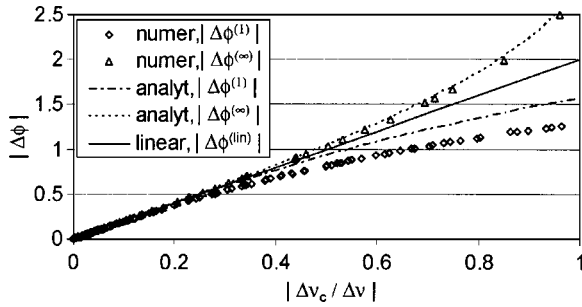


FIG. 2. Comparison of $\Delta\phi$ vs $\Delta\nu_c/\Delta\nu$ between numerical simulations and Eqs. (35), (38), and (39).

$$\Delta\phi^{(1)} \approx 2 \arctan\left(\left|\frac{d\phi}{d\nu}\right|_{\nu_c} \frac{\Delta\nu_c}{2}\right). \quad (35)$$

2. Phase shift for ∞ periods

For a structure with ∞ resonator periods, the linear phase relation is given by Eq. (15)

$$\phi_L^{(\infty)}(\nu) = \pm \frac{\pi}{2} - \arcsin\left[\left|\frac{d\phi_L}{d\nu}\right|_{\nu_{c,L}} (\nu - \nu_{c,L})\right]. \quad (36)$$

Again neglecting the resonance bandwidth change, one immediately obtains for the nonlinear phase relation

$$\phi_{NL}^{(\infty)}(\nu) = \pm \frac{\pi}{2} - \arcsin\left[\left|\frac{d\phi}{d\nu}\right|_{\nu_c} (\nu - \nu_{c,NL})\right], \quad (37)$$

since no problems arise with transmission here. Note that in the bistable region of course two phase relations exist: The “transmissive” one is given here, the other one is simply $\phi_{NL}^{(\infty)}(\nu) = \pi$ if $n_2 > 0$ and $\phi_{NL}^{(\infty)}(\nu) = 0$ if $n_2 < 0$. So $\Delta\phi^{(\infty)}$ is equal to

$$\Delta\phi^{(\infty)} = 2 \arcsin\left(\left|\frac{d\phi}{d\nu}\right|_{\nu_c} \frac{\Delta\nu_c}{2}\right). \quad (38)$$

3. Comparison and generation

If small resonance shifts or large resonance bandwidths (which means a small value of $|d\phi/d\nu|_{\nu_c}$) are assumed, Eqs. (35) and (38) can be linearly approximated as

$$\Delta\phi^{(\text{lin})} = \left|\frac{d\phi}{d\nu}\right|_{\nu_c} \Delta\nu_c, \quad (39)$$

which means that this $\Delta\phi^{(\text{lin})}$ will also be approximately valid for any finite number of periods N . Note that this formula for the phase shift $\Delta\phi$ is completely in accordance with intuitive reasoning: a phase shift proportional to $\Delta\nu_c$ and to $|d\phi/d\nu|_{\nu_c}$ is indeed what one would expect.

To check these results, the phase shift $\Delta\phi$ is plotted as a function of the relative resonance shift $\Delta\nu_c/\Delta\nu (=|d\phi/d\nu|_{\nu_c}\Delta\nu_c/2)$ for a large variation of all parameters (N_{dbr} , N_{cav} , n_b/n_a , n_2 , and $|E_{\text{in}}|$) in Fig. 2. The numerical simulations were obtained by means of a nonlinear extension,¹² of cavity modeling framework¹³ (CAMFR) based on spatial index discretization.

As can be seen, excellent agreement is obtained between numerical simulations and the analytical formulae (35), (38), and (39) for all situations. This also verifies the theory of Sec. IV B. The deviations between simulations and Eq. (35) in the case of one period are due to transmission issues, as discussed in Sec. IV B 1.

C. Complete Kerr-nonlinear resonator (modal approach)

As discussed in Sec. IV A 2, the resonance shift of a complete Kerr-nonlinear structure cannot easily be derived starting from Eq. (22). However, instead of calculating first the resonance shift and using that result to determine the phase shift—as done in Sec. IV B, $\Delta\phi$ can be calculated immediately, using modal theory.

In modal theory, the nonlinear field profile along the propagation axis is assumed to stay close to the linear one, so that the nonlinear action only consists of changing the amplitude of this profile.¹⁴ It is obvious that a modal approach will only be valid for small nonlinearities, which is in general the case for Kerr-nonlinear effects. Using the general theory in Ref. 14 and the intermediate results in Ref. 6, one immediately obtains for the (linearized) single period phase change $\Delta\phi^{(\text{lin})}$

$$\Delta\phi^{(\text{lin})} \approx \frac{3\pi}{8} \left(\frac{n_{a,0}}{n_{b,0}}\right)^{2N_{\text{dbr}}} \frac{n_2}{n_{a,0}} |E_{\text{in}}|^2 \left(N_{\text{cav}} + \frac{n_{a,0}^4 + n_{b,0}^4}{n_{a,0}^4 - n_{b,0}^4}\right), \quad (40)$$

in the case of $n_{a,2} = n_{b,2} = n_2$ and $n_{a,0} > n_{b,0}$, as considered in this paper. It is however easy to extend the calculation to more general cases, such as $n_{a,2} \neq n_{b,2}$. The main disadvantage of a modal approach is that it is quite difficult to gain simple insights in the nonlinear interactions, such as Eq. (39).

Using Eqs. (35), (38), and (39) and the theory of Sec. IV B 3, the phase changes for complete Kerr-nonlinear resonator structures, consisting of one and ∞ periods, are then

$$\Delta\phi^{(1)} \approx 2 \arctan\left[\frac{3\pi}{16} \left(\frac{n_{a,0}}{n_{b,0}}\right)^{2N_{\text{dbr}}} \frac{n_2}{n_{a,0}} |E_{\text{in}}|^2 \times \left(N_{\text{cav}} + \frac{n_{a,0}^4 + n_{b,0}^4}{n_{a,0}^4 - n_{b,0}^4}\right)\right], \quad (41)$$

$$\Delta\phi^{(\infty)} \approx 2 \arcsin\left[\frac{3\pi}{16} \left(\frac{n_{a,0}}{n_{b,0}}\right)^{2N_{\text{dbr}}} \frac{n_2}{n_{a,0}} |E_{\text{in}}|^2 \times \left(N_{\text{cav}} + \frac{n_{a,0}^4 + n_{b,0}^4}{n_{a,0}^4 - n_{b,0}^4}\right)\right]. \quad (42)$$

Now, based on Eq. (39), it is also possible to determine the resonance shift $\Delta\nu_c$ analytically for a complete Kerr-nonlinear resonator

$$\Delta\nu_c = -\frac{3}{4} \left(\frac{n_{a,0}}{n_{b,0}} \right)^{N_{\text{dbr}}} |E_{\text{in}}|^2 \frac{n_2}{n_{a,0}} \nu_c \frac{N_{\text{cav}} + \frac{n_{a,0}^4 + n_{b,0}^4}{n_{a,0}^4 - n_{b,0}^4}}{N_{\text{cav}} + \frac{n_{b,0}}{n_{a,0} - n_{b,0}}}. \quad (43)$$

Note the close resemblance of this equation with Eq. (29). As predicted in Sec. IV A 2, one indeed has, $\Delta\nu_c \rightarrow -(3/4) \times (n_{a,2}/n_{a,0})(n_{a,0}/n_{b,0})^{N_{\text{dbr}}} |E_{\text{in}}|^2 \nu_c$ for large cavities.

V. DESIGN AND DISCUSSION

As mentioned in the Introduction, the design of a resonating structure for Kerr-nonlinear phase shifting will be a tradeoff among input power, device length, and signal bandwidth.

Since the resonance peaks in the linear and the nonlinear case do not coincide, the signal bandwidth $\Delta\nu_s$ can be substantially lower than the resonance bandwidth $\Delta\nu$. In the ideal case, $\Delta\nu_s$ will be equal to the bandwidth overlap between both cases, thus,

$$\Delta\nu_s = \Delta\nu - \Delta\nu_c. \quad (44)$$

In the case of a realistic, finite structure, the resonance window will, in fact, not be completely transmissive. At the edges, the transmission function will show a number of peaks (increasing with the number of periods), in between which the transmission can drop even more than 50%, depending on the index contrast of the mirrors. Therefore, $\Delta\nu$ should be correct with a factor $f_{\text{corr}} < 1$, so the maximum signal bandwidth is

$$\Delta\nu_s = f_{\text{corr}} \Delta\nu - \Delta\nu_c. \quad (45)$$

A good estimate for this correction factor was found to be $f_{\text{corr}} = 0.5$. This value was obtained by comparing the high transmission shape of general, multiperiod resonator structures ($N=3-9$) with their resonance bandwidth $\Delta\nu$.

From Eqs. (39), (14), (43), and (45), this tradeoff is obvious; to minimize the device length L_{tot} the phase shift per unit of length $\Delta\phi/L_{\text{per}}$ must be maximized. This implies that the resonance shift $\Delta\nu_c$ should be as high and the resonance bandwidth $\Delta\nu$ as low as possible. However these last two conditions also result in a lower signal bandwidth $\Delta\nu_s$. Furthermore, a restriction to the resonance shift $\Delta\nu_c$ will be imposed by the achievable input power.

This optimization is now done for a realistic example: a coupled cavity photonic wire in silicon-on-insulator (SOI) is

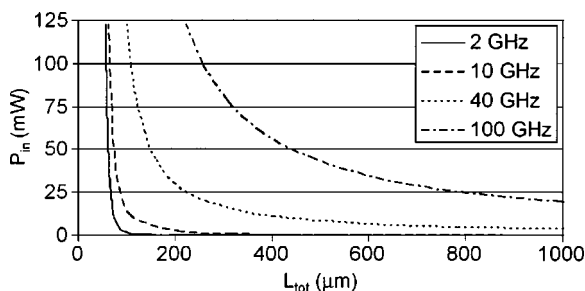


FIG. 3. Input power P_{in} required to obtain a nonlinear phase shift of π by propagation through a resonator-based distance of L_{tot} for several signal bandwidths.

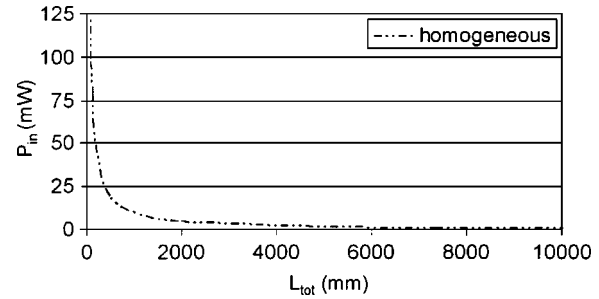


FIG. 4. Input power P_{in} required to obtain a nonlinear phase shift of π by propagation through a homogeneous distance of L_{tot} .

approximated by taking $n_a = 2.6$ and $n_b = 2.36$, which corresponds to an index contrast of $\approx 10\%$. The Kerr coefficient is equal to $n_2 = 0.6 \times 10^{-13} \text{ cm}^2/\text{W}$ (or $2.4 \times 10^{-16} \text{ cm}^2/\text{V}^2$) and the cross-section area $A_{\text{cross}} \approx (\lambda_c^2/2n_a)$. The input power P_{in} corresponding to a certain input field E_{in} may be estimated from the input intensity $I_{\text{in}} = (1/2)cn_a\epsilon_0|E_{\text{in}}|^2$ and the cross-section area, so

$$P_{\text{in}} \approx I_{\text{in}} A_{\text{cross}} = \frac{c}{8n_a} \epsilon_0 \lambda_c^2 |E_{\text{in}}|^2. \quad (46)$$

The results are shown in Fig. 3; the required input powers which may be expected are shown as a function of device length for several signal bandwidths. To become continuous curves, the parameters N_{dbr} and N were assumed to be continuous, which is a good approximation since both values are typically high. The situation of a simple wire without resonating structures is drawn in Fig. 4 as a comparison.

Comparing Figs. 3 and 4, it can be seen that the improvements in the order of 10 000 for the device length are possible (depending on the signal bandwidth). The signal bandwidth is however an important limiting factor, especially for very high band rates. Note also that from a certain input power on, the relative improvement of L_{tot} drops very steeply so using even higher powers are not sound.

In Fig. 5, the example above is recalculated with other index contrasts for a signal bandwidth of 40 GHz. From this, it is clear that high index contrasts allow major improvements in the device length. This is due to two factors: first, the length of mirrors with the same reflectivity substantially reduces for higher contrast [Eq. (5)]. In addition, the resonance shift for a certain input power will also be larger for shorter mirrors, because a smaller part of the nonlinear phase change in the cavity will be used to compensate the phase

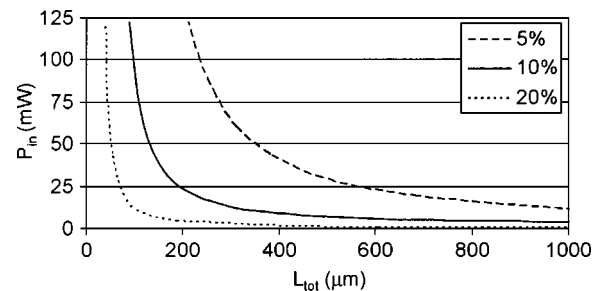


FIG. 5. Influence of index contrast on the $P_{\text{in}}-L_{\text{tot}}$ tradeoff, shown in Fig. 3, for the case of 40 GHz.

TABLE I. Best parameter values to minimize the device length for $\Delta\nu_s = 10$ GHz and $P_{in} < 30$ mW.

	N_{dbr}	N_{cav}	N	P_{in} (mW)	L_{tot} (μm)
1	54	2	5	29.724	87.188
2	54	3	5	25.921	88.678
3	56	1	5	22.856	88.843
4	54	4	5	22.981	90.168
5	56	2	5	19.502	90.334

shift in the mirrors, as discussed in Sec. IV A 1. The obtainable index contrast is however typically limited by scattering and radiation loss in actual structures.

An important remark is that for all situations depicted in Figs. 3 and 5, one has $N_{cav}=1$. From Eqs. (14) and (16), it can be seen that the resonance bandwidth reduces both with higher $|r_{dbr}|_{\nu_c}$ and larger N_{cav} . However, only the mirror strength determines the field strength inside the cavity [Eq. (25)]. On the other hand, a larger cavity improves the frequency shift, as mentioned in Sec. IV A 1. These results now imply that increasing $|r_{dbr}|_{\nu_c}$ is more efficient in terms of device length than increasing the cavity length.

To determine the real optimum, only integer values of N_{dbr} and the period number N can be taken into account. In most situations, one will also choose N_{dbr} to be even (this was implicitly done in Sec. II). Otherwise $b_{\lambda/8}$ layers must be constructed at the in- and out-coupling sections, which require more demanding feature size limitations. Suppose one would like to minimize the device length for a signal bandwidth of 10 GHz and input powers up to 30 mW is allowed. To find the optimal solution, one should first make a 3D graph of the input power P_{in} required for $N\Delta\phi = \pi$ with discrete axis N_{cav} , N_{dbr} , and N under the condition that $\Delta\nu_s = 10$ GHz. Then solutions can be found by transferring the cut $P_{in} \leq 30$ mW to a new 3D graph now showing L_{tot} . The five best parameter combinations obtained in this way are shown in Table I, together with the required input power P_{in} and the total device length L_{tot} .

Note that N_{cav} is not necessarily equal to one, since only discrete solutions are now taken into account. Note also that the required input power already drops 10 mW for an increase in device length of 3 μm . Due to tradeoff requirements, several solutions are found, which lie very close together.

To clarify this even further, $\Delta\phi/L_{per}$ is drawn as a function of N_{dbr} and N_{cav} in Fig. 6. The limiting line $P_{in} = 30$ mW is also shown.

From this figure, it can be seen that $\Delta\phi/L_{per}$ is almost constant along $P_{in} = 30$ mW for low N_{cav} . Only for increasing N_{cav} , $\Delta\phi/L_{per}$ drops more substantially. As already discussed, increasing $|r_{dbr}|_{\nu_c}$ (thus N_{dbr}) is more efficient in terms of device length than increasing N_{cav} . However for low cavity values, this difference in efficiency is relatively low, since increasing N_{cav} still improves the frequency shift substantially (Sec. IV A 1). Discreteness of the parameter space therefore allows closely spaced optimal solution.

The optimal result of Table I is now numerically checked in Fig. 7.

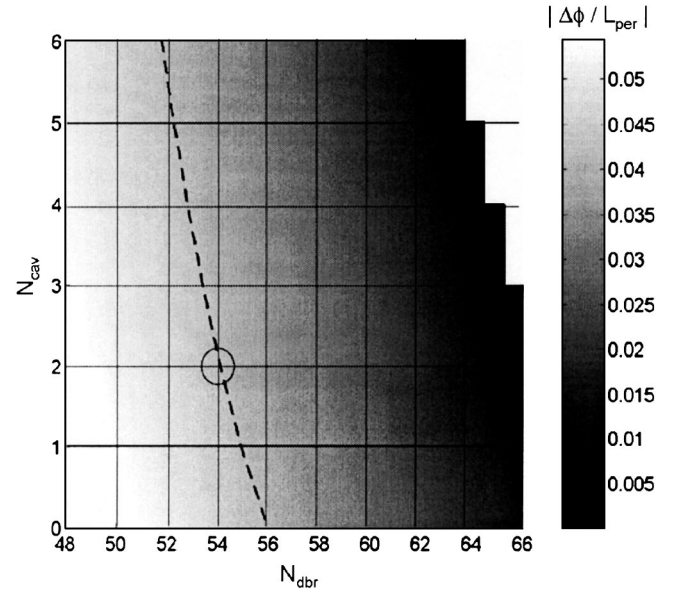


FIG. 6. Phase shift per unit of length $\Delta\phi/L_{per}$ as a function of N_{cav} and N_{dbr} . The line $P_{in} = 30$ mW is also shown.

It can be seen that the resonance shift is equal to 0.19 nm, which is in good agreement with Eq. (43). The obtained phase shift for $\lambda = 1/2(\lambda_{c,L} + \lambda_{c,NL}) = 1.550095 \mu\text{m}$ is $\Delta\phi_{tot} \approx 3.32$, which is close to π . As can be seen, the phase shift is almost constant over a large range, however, for resonance of transmission, the usable wavelength range ($|t_{tot}|^2 > 0.9$) is only $\Delta\lambda_s = 0.085$ nm, so the signal bandwidth is approximately limited to 10 GHz, as expected.

The resonance bandwidth based on Eqs. (14) and (16) is $\Delta\lambda = 0.6$ nm, so the resonance shift is about one third of the bandwidth. On the other hand, $|d\phi/d\nu|_{\nu_c}$ is also much steeper than in the absence of resonators. This means that both $|d\phi/d\nu|_{\nu_c}$ and $\Delta\nu_c$ are important in this example. For higher P_{in} or n_2 , the driving factor of the phase shift will typically be $\Delta\nu_c$ ($\Delta\nu_c \approx f_{corr}\Delta\nu$), while in the case of lower n_2 or P_{in} , $|d\phi/d\nu|_{\nu_c}$ will be more significant ($\Delta\nu_c \ll f_{corr}\Delta\nu$).

VI. CONCLUSIONS

In this paper, the design of ultrafast nonlinear phase shifting devices by means of resonators has been discussed. It has been shown that a phase shift of π can be achieved

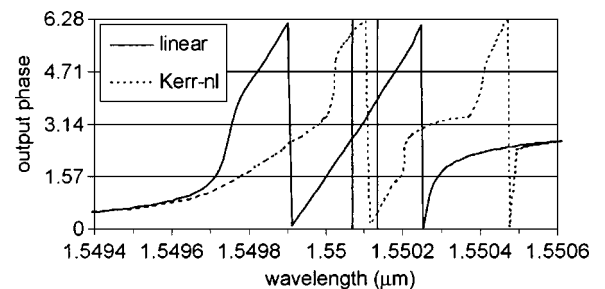


FIG. 7. Numerical calculation of the linear and nonlinear phase relations $\phi_L(\lambda)$ and $\phi_{NL}(\lambda)$. The structural parameters of the resonator are $n_a = 2.6$, $n_b = 2.36$, $N_{dbr} = 54$, $N_{cav} = 2$, $N = 5$, and $\lambda_c = 1.55 \mu\text{m}$, while the nonlinear input power is given by $P_{in} = 29.24$ mW. The signal bandwidth is indicated by vertical lines.

within reasonable power and device length budgets, much smaller compared to the case of simple waveguides.

It was, in particular, shown that device optimization is possible by using resonators consisting of high contrast mirrors, both for reducing the optical power and the device length. Furthermore, the cavity length itself should be kept small, although not necessarily a half wavelength.

An important limitation to this concept is however the signal bandwidth. A high bandwidth signal (>100 GHz) requires substantially more optical power or longer nonlinear components.

ACKNOWLEDGMENTS

Part of this work was performed in the context of the Belgian DWTC IAP-PHOTON project, Two of the authors

(G.P.) and (P.B.) thank the Flemish Fund for Scientific Research (FWO-Vlaanderen) for a doctoral and a postdoctoral fellowship, respectively.

- ¹A. Melloni, F. Morichetti, and M. Martinelli, *Opt. Quantum Electron.* **35**, 365 (2003).
- ²J. E. Heebner and R. B. Boyd, *Opt. Lett.* **24**, 847 (1999).
- ³S. Blair, *Opt. Lett.* **27**, 613 (2002).
- ⁴D. Pelinovsky, J. Sears, L. Brzozowski, and E. H. Sargent, *J. Opt. Soc. Am. B* **19**, 43 (2002).
- ⁵J. He and M. Cada, *IEEE J. Quantum Electron.* **27**, 1182 (1991).
- ⁶U. Peschel, T. Peschel, and F. Lederer, *IEEE J. Quantum Electron.* **30**, 1241 (1994).
- ⁷S. Radic, N. George, and G. Agrawal, *J. Opt. Soc. Am. B* **12**, 671 (1995).
- ⁸J. Lee and G. P. Agrawal, *IEEE J. Quantum Electron.* **39**, 508 (2003).
- ⁹D. Weaire and J. P. Kermode, *J. Opt. Soc. Am. B* **3**, 1706 (1986).
- ¹⁰P. W. Smith and E. H. Turner, *Appl. Phys. Lett.* **30**, 280 (1977).
- ¹¹A. Yariv, Y. Xu, R. K. Lee, and A. Scherer, *Opt. Lett.* **24**, 711 (1999).
- ¹²B. Maes, P. Bienstman, and R. Baets, *Opt. Quantum Electron.* **36**, 15 (2004).
- ¹³<http://camfr.sourceforge.net/>
- ¹⁴T. Peschel and F. Lederer, *Phys. Rev. B* **46**, 7632 (1992).